Fusion neutron detector for time-of-flight measurements in *z*-pinch and plasma focus experiments

D. Klir,[1,a)] J. Kravarik,[1] P. Kubes,[1] K. Rezac,[1] E. Litseva,[1] K. Tomaszewski,[2] L. Karpinski,[3] M. Paduch,[3] and M. Scholz[3]
[1]*Faculty of Electrical Engineering, Czech Technical University in Prague, Technicka 2, 16627 Prague 6, Czech Republic*
[2]*ACS Ltd., Advanced Diagnostics Laboratory, Warsaw, Poland*
[3]*Institute of Plasma Physics and Laser Microfusion, Warsaw, Poland*

(Received 8 October 2010; accepted 2 February 2011; published online 11 March 2011)

We have developed and tested sensitive neutron detectors for neutron time-of-flight measurements in *z*-pinch and plasma focus experiments with neutron emission times in tens of nanoseconds and with neutron yields between 10^6 and 10^{12} per one shot. The neutron detectors are composed of a BC-408 fast plastic scintillator and Hamamatsu H1949-51 photomultiplier tube (PMT). During the calibration procedure, a PMT delay was determined for various operating voltages. The temporal resolution of the neutron detector was measured for the most commonly used PMT voltage of 1.4 kV. At the PF-1000 plasma focus, a novel method of the acquisition of a pulse height distribution has been used. This pulse height analysis enabled to determine the single neutron sensitivity for various neutron energies and to calibrate the neutron detector for absolute neutron yields at about 2.45 MeV. [doi:10.1063/1.3559548]

I. INTRODUCTION

Time-of-flight (ToF) diagnostics is one of the most accurate methods of measuring energy spectra of fast neutrons which are produced by D(d, n)^{3}He fusion reactions. That is why the ToF analysis has been applied to diagnose fusion processes in controlled thermonuclear fusion research.[1–4] This method is also commonly used for diagnostics of *z*-pinches and plasma foci with neutron yields between 10^6 and 10^{13} (see Refs. 5–12). Such neutron yields enable to acquire ToF signals within a single shot. The duration of neutron ToF signals in *z*-pinches is typically tens of nanoseconds; therefore, it is necessary to use neutron detectors with a fast time response. Nanosecond temporal resolutions can be easily achieved with plastic scintillators which are relatively inexpensive and easy to handle. These properties are important when a large number of ToF detectors are used, such as at the PF-1000 facility.[8] In this paper, we describe the design, the calibration, and the initial test of a neutron detector which is composed of the BC-408 fast plastic scintillator and the Hamamatsu H1949-51 PMT assembly. The description of the neutron detector is provided in Sec. II. Section III deals with the issues of temporal resolution and timing of the detector. Section IV presents a novel method of the measurement of single neutron sensitivity in the energy range between 1.8 and 3.0 MeV. Section V brings forward the calibration of the neutron detector for absolute neutron yields at 2.45 MeV. Finally, Sec. VI describes the initial test of the neutron ToF detector during the measurement of a neutron production time.

II. DESCRIPTION OF NEUTRON TIME-OF-FLIGHT DETECTOR

One of the most common ways of detecting fusion neutrons is to produce a recoil proton through elastic scattering in a hydrogen-containing scintillator.[13] Because the free path length of recoil protons is usually negligible in comparison with scintillator dimensions, the recoil proton energy is fully deposited into a scintillator. The fluorescence of excited atoms in a scintillator can be converted into an electrical pulse by a PMT combined with a high-bandwidth transient digitizer. For purposes of ToF analysis with the temporal resolution on the order of several nanoseconds, fast plastic scintillators based on a polyvinyltoluene matrice are used since they can be easily fabricated and handled. In our plasma focus and *z*-pinch experiments,[8,10,12,14] we mostly used Saint Gobain BC-408 plastic scintillators with a 0.9 ns rise time, a 2.5 ns FWHM, a 2.1 ns decay time, and a 425 nm peak emission wavelength.[15] The general characteristics of the BC-408 scintillator are the density of 1.032 g/cc and the atomic ratio between hydrogen and carbon of 1.104. The front surface of our cylindrical scintillator is 45 mm in diameter. The 50 mm thickness of the scintillator is approximately equal to the mean free path of 2.45 MeV neutron in the polyvinyltoluene matrice. The fast plastic scintillator is coupled to the Hamamatsu H1949-51 PMT assembly which is composed of a high voltage divider and the R1828-01 photomultiplier tube.[16] This type of the PMT with a 1.3 ns rise time (at a 2.5 kV voltage), the peak cathode sensitivity at 420 nm and the photocathode of a 46 mm effective diameter is well matched to the parameters of the scintillator. A large dynamic range of the PMT ($>10^6$, see Ref. 17) enables us to use a neutron detector for a broad range of neutron yields. The neutron detector described in this paper was used at small plasma foci with 10^6 neutrons/shot,[10,11] at the mega-ampere PF-1000 plasma focus[8,36] and the S-300

a)Electronic mail: daniel.klir@fel.cvut.cz.

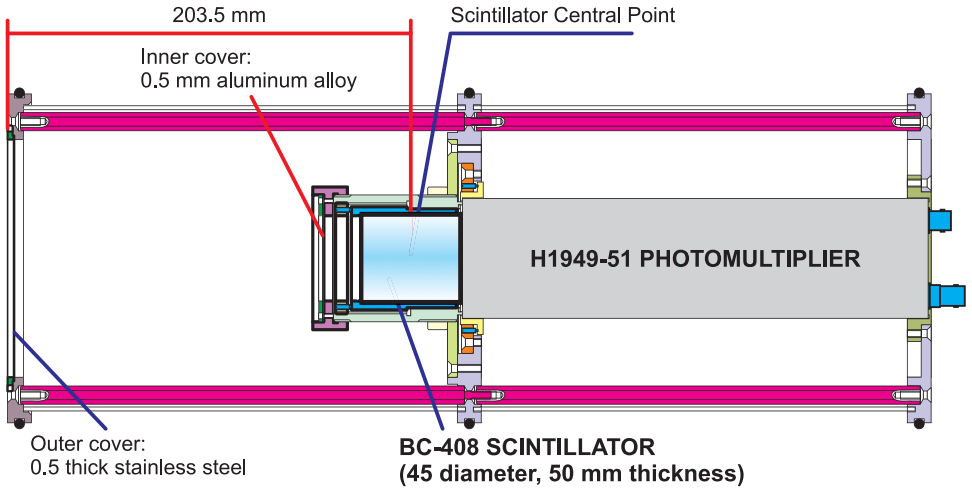

FIG. 1. (color online) Cross section of the neutron time-of-flight detector showing the BC-408 scintillator and the H1949-51 photomultiplier tube inside the stainless-steel housing. The inside cover of the scintillator is from black-anodized aluminum. In order to minimize the interface reflection, a silicone grease was applied between the scintillator and the PMT entrance window.

z-pinch[12] with neutron yields up to 10^{12} as well as at the PALS laser facility.[20]

As far as the electromagnetic shielding is concerned, each scintillator-PMT combination was put inside a heavy duty housing which was manufactured by ACS Ltd.[18] (see Fig. 1). At the PF-1000 facility, the housing with the detector was placed into a AS16U-8 mobile stand at 1.2 m above the floor.[19] In the presence of a harsh x-ray environment, such as at the S-300 z-pinch[12] or the PALS laser system,[20] scintillators were shielded with up to 10 cm of lead. It was also suitable to place the scintillator-PMT combination in such a position to avoid a direct exposure of the photomultiplier tube or to shield the PMT by even larger amount of lead or tungsten. In both cases, it was essential to place shielding close to the neutron detector in order not to influence significantly the time-of-flight of neutrons. Further details on the design of the ToF detector can be found in Ref. 18.

III. TEMPORAL RESOLUTION AND TIMING CALIBRATION

The temporal resolution of the neutron detector is given by the pulse width of the scintillator (2.5 ns FWHM) and by the width of a PMT time response which depends on a photomultiplier voltage (cf. Fig. 2). The response of an acquisition system below 1 ns and a transit time of 2.5 MeV neutrons through 50-mm-thick scintillators (1 ns uncertainty) do not limit the temporal resolution. For the most commonly used PMT voltage of 1.4 kV, the typical time response to a 3 MeV neutron recorded with a 500 MHz oscilloscope is shown in Fig. 3. The observed signal corresponds to the result obtained by the convolution of the PMT time response with the scintillator decay (see a dashed line in Fig. 3). The width (FWHM) of the neutron signal was 5.7 ± 0.6 ns ($\pm 2\sigma$). The rise time and fall time were 2.9 ± 0.2 and 8 ± 1 ns, respectively. As far as the detection of two neutrons is concerned, it was possible to distinguish them when the temporal shift was about 5.5 ns.[18] The temporal resolution could be slightly improved by a higher PMT voltage. At a 1.9 kV voltage, for example, the width of the neutron signal was by 0.4 ns smaller, i.e., 5.3 ns. (At even higher voltages, a single neutron produces >10 mA peaks and, if a large number of neutrons are detected, the PMT may operate in a nonlinear regime, i.e., the anode current is above 250 mA. For that purpose, a neutral density filter may be placed between the scintillator and the PMT. Because it reduces the signal-to-noise ratio, we do not use operating voltages above 2.0 kV.)

The applied voltage determines not only what the temporal resolution shall be but also influences a PMT delay, the information that is necessary to know in order to synchronize all neutron detectors between each other as well as with other diagnostic tools. The dependence of the PMT delay on the applied voltage was measured for each PMT and the result of one of PMTs can be seen in Fig. 4. An uncertainty of the PMT delay was below 1 ns and differences between various PMTs did not exceed 2 ns for >1 kV voltages.

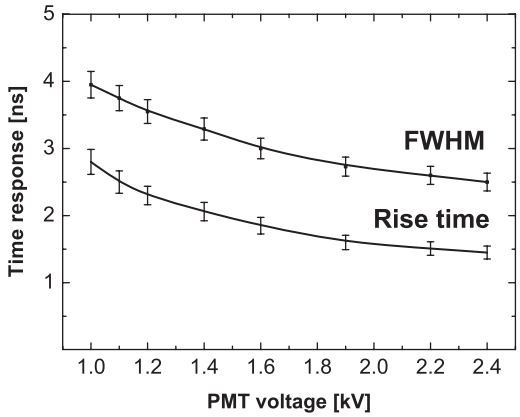

FIG. 2. The dependence of the PMT response (FWHM and rise time) on the operating voltage. The error bars indicate $\pm 2\sigma$ uncertainty.

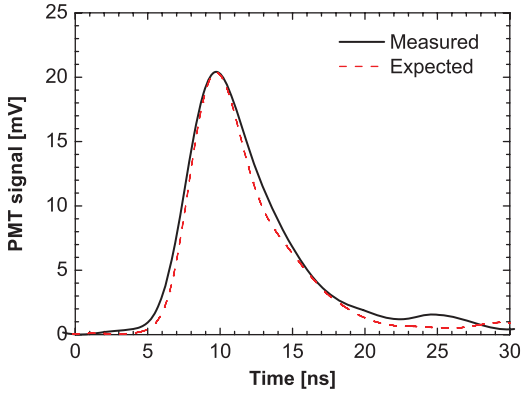

FIG. 3. (color online) The typical time response to a 3 MeV neutron recorded with a 500 MHz oscilloscope (solid line) and the convolution of the PMT time response with the scintillator decay (dashed line). The measurement was based on the technique which is described in Sec. IV. Since only a single neutron was detected, the uncertainty caused by a neutron transit time through 50-mm-thick scintillators is not included in this time response.

IV. LIGHT OUTPUT AND SINGLE NEUTRON SENSITIVITY

The pulse height distribution for a specific scintillator and for various neutron energies can be calculated by the MCNP code[21] postprocessed by the PoliMi package, similarly as it was simulated by Pozzi *et al.*[22,23] Such a numerical simulation is useful for a calibration of detectors operating in the counting mode. In the case of our ToF measurements,[8,12,24] the detectors are operating in the current mode. It means that a large number of neutrons create a ToF signal. Therefore, it is necessary to know what the average light output for neutrons with a given time-of-flight is.

The calculation of the average light output for neutron energies between 1.8 and 3.0 MeV is not as straightforward as it may seem. First, recoil proton energies are distributed uniformly from zero energy to the full kinetic energy of an incident neutron.[13] Second, the response to protons and carbons is nonlinear for energies below 5 MeV.[15,25] Third, neutrons can lose their kinetic energy during the transport from the source to the detector. If a neutron loses its energy near the scintillator (especially at the PMT and lead shielding), the measured time-of-flight corresponds to a higher neutron energy than the energy of a detected neutron. Finally, it is necessary to calculate the coupling efficiency of a scintillator light by the PMT tube, the photocathode quantum efficiency, and the electron gain.

To include all these effects, we developed a novel method of calibrating a neutron detector for different neutron energies between 1.8 and 3.0 MeV. We experimentally estimated *in situ* the response to a single neutron at the PF-1000 plasma focus (2 MA peak current, 5 μs rise time, Ref. 26). It means that the detector described in this paper was developed for the application at this device. When a deuterium gas is used, this facility is capable to produce more than 10^{11} D(d, n)^{3}He neutrons with energies from 1.8 to 3.5 MeV within 100 ns. In the case of such a high neutron yield, it is possible to detect individual neutrons at a distant place from the neutron source and to calculate the energy of a detected neutron by the ToF method. An illustrative ToF signal is displayed in Fig. 5. In comparison with the method described in Refs. 27 and 28, where the neutron detector was calibrated at a 2 m distance, the detector at the PF-1000 was positioned upstream at a distance of 83.7 m from the plasma. Such a great distance enables us to measure the single neutron sensitivity for neutron energies between 1.8 and 3.0 MeV.

The kinetic energy of a neutron, E, could be calculated from the basic time-of-flight method. The energy resolution of the ToF method ΔE is determined mainly by the duration of neutron emission $\Delta\tau$ as

$$\frac{\Delta E}{E} = \frac{2\Delta\tau}{\tau}, \tag{1}$$

where τ is the neutron time-of-flight from a source to a detector. At the PF-1000 plasma focus, the FWHM of neutron emission $\Delta\tau$ is usually below 100 ns. Then, for a 83.7 m distance and for 2.45 MeV neutron with the ToF of 3860 ns, we obtain the uncertainty of a neutron energy ΔE on the order of 0.1 MeV.

If the energy estimated from the time-of-flight is known, it is possible to measure a pulse height response of the detector to neutrons with various neutron energies. During the calibration at the PF-1000 facility, the noise level was 0.2 mV (root mean square). Therefore, the discrimination level was set at 1 mV and only single peaks above this threshold were taken into account. The response to a single neutron was

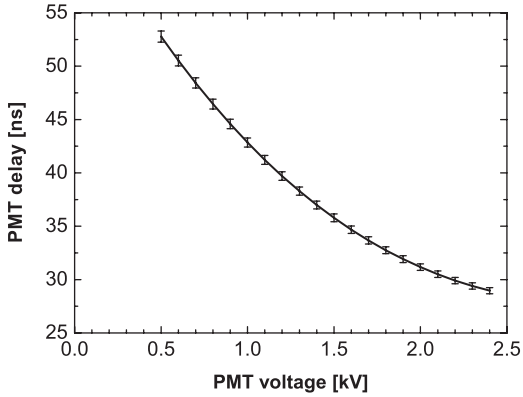

FIG. 4. The dependence of the PMT delay on the PMT voltage. The error bars indicate $\pm 2\sigma$ uncertainty.

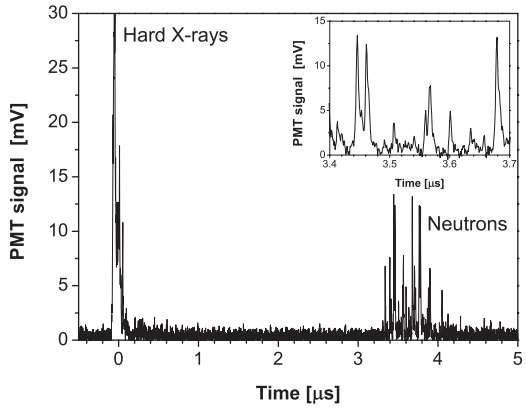

FIG. 5. An example of a ToF signal recorded at 83.7 m.

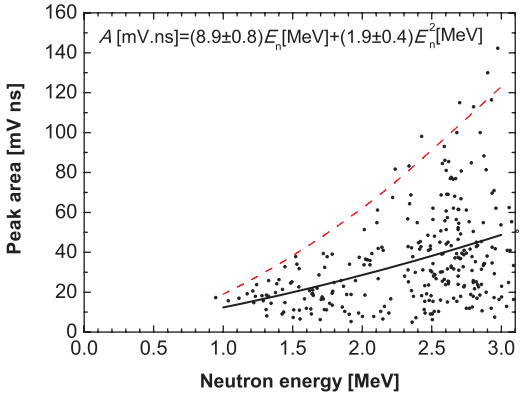

FIG. 6. (color online) The dependence of peak areas on neutron energies calculated from the neutron ToF. A dashed line represents a relative dependence of the light output for recoil protons according to Ref. 15.

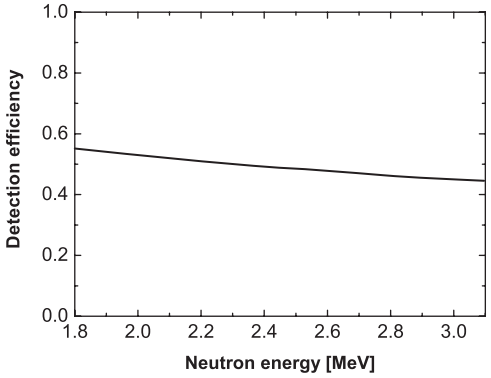

FIG. 7. The dependence of the detection efficiency of the neutron energy for 50 mm thick BC-408 scintillator.

recognized by its FWHM which should be between 5 and 7 ns. In order to avoid pile-up effect, we excluded from the analysis those parts of a ToF signal where the coincidence of two neutrons was expected. During 20 shots (these correspond to 1 day operation of the PF-1000 facility), we accumulated ~5000 peaks and analyzed 300 well separated peaks (see Fig. 6). Even though the operating regime of the PF-1000 facility was not optimized for the pulse height analysis and neutron yields were higher than optimal, 300 well separated pulses ensured sufficient accuracy for our Monte Carlo reconstruction of neutron energy spectra.[12,24,29,30] If a higher accuracy is required, more shots in an optimized regime of the device can be easily achieved.

Figure 6 shows that the maximum light output observed for a given energy of the incident neutron is rising more than linearly. Such a result agrees with the fact that the response to recoil protons with the full neutron energy is nonlinear for energies below 5 MeV.[13,15,25] Since only a portion of the neutron energy is usually transferred to a recoil proton in a single scattering event, there are more events with pulse heights lower than the maximum for the incident neutron energy in Fig. 6. As far as the average values are concerned, the dependence of the light output on the neutron energy was fitted by a polynomial of the second order. The result was influenced by the 1 mV discrimination level because events with 0–5 mV ns peak areas were not included and, thus, the average light output is somewhat overestimated. If we assume that a number of events in the 0–10 mV ns region was the same as in the 10–20 mV ns region, the average neutron light yield should be decreased by about 3 mV ns for all energies and we receive fit parameters which are presented in Fig. 6. Error estimates of fit parameters include the uncertainty of neutron energies and the influence of a discrimination level and Poisson statistics.

On the one hand, Fig. 6 shows that colliding neutrons with higher energies produce higher light outputs. But on the other hand, more energetic neutrons have usually lower probability of a scattering event with protons in a scintillator. In order to include this effect in our measurement with the BC-408 scintillator, we estimate the dependence of the detection efficiency on a neutron energy using the ENDF database.[31] In the first order approximation, we assume a thin target and we calculate the probability of the elastic interaction of an incident neutron with a recoil proton. The result can be seen in Fig. 7. Since the detection efficiency is not so strongly dependent on a neutron energy and since the light output caused by scattering on carbon is very small and can be neglected (cf. Ref. 15), the error of our approximation is expected to be on the order of a few percent. As a result, the detector sensitivity to multiple neutrons with various energies is given by the multiplication of the dependencies presented in Figs. 6 and 7.

Such a calibration of the current mode neutron ToF detector does not occur often in fusion experiments. Usually, the detector response is assumed to be independent on a neutron energy. This assumption is valid only in the case of a narrow neutron energy spectrum. In the case of z-pinch and plasma focus experiments,[5,12,24,32,33] the width of neutron energy spectra could exceed 500 keV and thus the dependence of a detector sensitivity on a neutron energy should be taken into account. For instance, the difference between 2.1 and 2.9 MeV neutrons reaches 35%. Such a value is comparable with the axial neutron emission anisotropy observed in z-pinches.[24]

V. NEUTRON YIELD AND NUMBER OF DETECTED NEUTRONS

The calibration mentioned in Sec. IV was carried out mainly for the purpose of more precise reconstruction of neutron energy spectra.[24,29,30] In addition to that, the known response of the detector to a single neutron can be used for the estimation of the number of detected neutrons by the current mode detector. Figure 8 shows the histogram of a peak area for neutrons with energies between 2.2 and 2.7 MeV. The average peak area A was about (37 ± 5) mV ns, i.e., 0.75 pC, for the 1.4 kV operating voltage (as regards the calibration at various voltages, it was possible to use the measured dependence of the radiant sensitivity of the PMT tube on a voltage published in Ref. 18). Then, if we determine the charge produced by the current mode detector, Q, the number of detected neutrons can be estimated as $N_{\text{detected}} = Q/A$.

If the number of detected neutrons is known, a neutron ToF detector can be calibrated for absolute neutron yields.

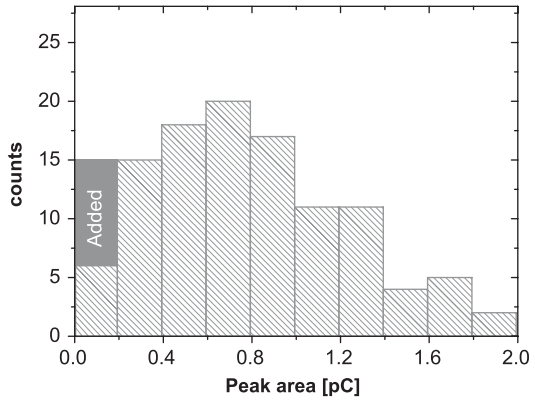

FIG. 8. The histogram of peak areas for 2.2–2.7 MeV neutrons. In order to include the effect of the discrimination limit, several counts were added into a 0–0.2 pC region.

Assuming the isotropic emission, the neutron yield is given by

$$Y = \frac{4\pi}{\Omega}\frac{N_{\text{detected}}}{\eta}, \tag{2}$$

where Ω and η stand for the solid angle and the efficiency of neutron detection, respectively. The solid angle Ω covered by a detector can be simply inferred from the experimental arrangement. As for the detection efficiency, η, i.e., the ratio between detected and impinging neutrons, it is ~50% in the case of 2.45 MeV neutrons (cf. Fig. 7). At the PF-1000, we were able to compare the neutron yield measured by this technique with the one determined by four silver activation detectors.[34] When we considered the influence of neutrons scattered at the experimental chamber (see Ref. 35 and 37), the neutron yields measured by scintillators were by about 30% lower. The observed difference could be ascribed to a neutron flux anisotropy and to the accuracy of neutron yield measurements by these methods.

On the contrary, if the neutron yield Y is known, we can calculate the expected number of detected neutrons N_{detected}. At the PF-1000 facility, for instance, neutron yields are on the order of 10^{11} per one shot. At the distance of 30 m, the 4.5 cm diameter of the cylindrical detector corresponds to the solid angle Ω of 2×10^{-7} srad. Calculating with the 50% detection efficiency, we obtain more than 7000 detected neutrons. As far as the number of detected neutrons is concerned, a neutron detector operating in the current mode requires a sufficiently high number of scattering events in order to reduce the quantum noise. The quantum noise is given not only by the stochastic nature of neutron detection but also by the stochastic transfer of a neutron energy to recoil protons and, therefore, by the stochastic distribution of pulse heights for a given neutron energy. Therefore, it is necessary for ToF measurements to detect at least several tens of neutrons within the temporal resolution of the detector. At the PF-1000 facility, the typical duration of ToF signals at 30 m is about 300 ns.[8] In the case of 7000 detected neutrons, we obtain about 115 neutrons within the 5 ns temporal resolution. Such a value seems to be high enough to reduce the quantum noise. In the case of the 85 m distance, the quantum noise is much more significant since the number of detected neutrons is lower and also the width of a ToF signal is broader. For this reason, it seems better to use cylindrical scintillators with a larger diameter.[18] Another possibility is to use a longer cylindrical scintillator positioned perpendicularly to the source–detector axis.

VI. TIME OF NEUTRON PRODUCTION, TEMPORAL ACCURACY, AND TEMPORAL RESOLUTION

An illustrative test of the fast neutron detector is the measurement of neutron production time at a small plasma focus PFZ at the Czech Technical University in Prague. The time of neutron production is usually estimated from the nearest neutron ToF signals, therefore, it is convenient to place the neutron detector as close to the source as possible. The shortest possible distance is given by an experimental arrangement and by the fact that a neutron signal has to be temporally separated from hard x-ray emission or harsh electromagnetic noise. At the PFZ device, the time of neutron production is estimated from the nearest side-on ToF detector at about 150 cm from the plasma. The advantage of side-on detectors is usually less amount of hardware in the direction of diagnostic ports which implies a smaller influence of scattered neutrons.[14] Another advantage of side-on detectors is that neutron energy spectra are centered at about 2.45 MeV. Therefore, in order to obtain the temporal evolution of neutron emission, it is possible to shift the observed neutron signals by the time-of-flight of 2.45 MeV neutrons (69.4 ns in the case of 150 cm distance, 64.4 ns delay after hard x-rays). For example, Fig. 9 shows a radial neutron signal shifted by the ToF together with waveforms of soft and hard x-ray radiations and current derivative $\mathrm{d}I/\mathrm{d}t$.

In Fig. 9, we can see the temporal correlation of the $\mathrm{d}I/\mathrm{d}t$ dip (maximum compression) and soft and hard x-ray signals. All these waveforms were recorded by the same oscilloscope and were adjusted to account for different transit times from each detector. A 2 ns temporal uncertainty between these waveforms is given by the uncertainty of a detector distance, length of cables, a PMT delay, and a 500 MHz bandwidth of the oscilloscope. As regards the shift between hard x-rays and neutron signals, they are taken from the same waveform. Therefore, the temporal uncertainty is determined only by the accuracy of the distance from the source to the detector. In

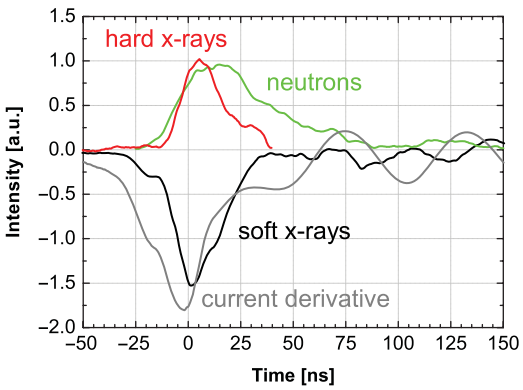

FIG. 9. (Color online) The waveforms of current derivative, soft x-rays, hard x-rays, and neutron emission recorded in discharge No. 090429-23 with a neutron yield of about 10^7.

the case of 2.45 MeV neutrons, the distance of about 2 cm corresponds to a 1 ns temporal uncertainty.

Much more important than the 2 ns temporal uncertainty (temporal accuracy) is the temporal resolution of neutron detection. Since the neutron emission is detected at a certain, nonzero, distance from the neutron source, the temporal resolution is given not only by the 5.7 ns pulse response of the neutron detector (see Sec. II), but also by the width of a neutron energy spectrum. The difference between neutron kinetic energies implies the broadening of ToF signals. In the case of a 500 keV width of side-on energy spectra which was observed in most of plasma focus and z-pinch experiments,[5,12,24,32] the instant neutron emission is broadened to a 6.5 ns FWHM at 1.5 m distance. Calculating with the 5.7 ns pulse response to a single neutron, we obtain the overall temporal resolution of about 8.5 ns.

The overall temporal resolution of 8.5 ns seems to be sufficient for most neutron measurements in gas puff z-pinches and plasma foci. In these devices, temporal changes of neutron emission are not so fast since it takes some time to produce fusion neutrons from accelerated deuterons. For instance, the free path length of 100 keV deuterons in z-pinch plasmas is typically several centimeters long. Each 3 cm then represents the time period of about 10 ns. This time delay can partly explain differences between the hard x-ray and neutron signal in Fig. 9. The application of a faster neutron detector is, therefore, valuable especially in the case of a shorter neutron emission, a narrow energy spectrum, and a small distance of the neutron detector.

VII. CONCLUSION

We have developed and tested sensitive neutron detectors which are designed for neutron ToF measurements in z-pinch and plasma focus experiments. The pulse response of the neutron detector is ~5 ns. During the calibration procedure at the PF-1000 facility, we demonstrated the applicability of a novel method of the acquisition of the pulse height distribution. With the ToF detector at the distance of 85 m, it was possible to measure the single neutron sensitivity for neutron energies between 1.8 and 3.0 MeV. The detector described in this paper has been successfully used in z-pinch and plasma focus experiments with neutron yields from 10^6 to 10^{12} neutrons/shot.

ACKNOWLEDGMENTS

This research has been supported by Grant Nos. 202-08-P084, 202-08-H057 of the Grant Agency of the Czech Republic, by research program Nos. LA08024, ME09087, LC528 of the Ministry of Education, by IAEA Grant No. RC14817 and CTU Grant No. SGS10/266/OHK3/3T/13.

[1] O. N. Jarvis, Plasma Phys. Controlled Fusion **36**, 209 (2010).
[2] T. Elevant, P. van Belle, O. N. Jarvis, and G. Sadler, Nucl. Instrum. Methods Phys. Res. A **364**, 333 (1995).
[3] R. A. Lerche, V. Yu. Glebov, M. J. Moran, J. M. McNaney, J. D. Kilkenny, M. J. Eckart, R. A. Zacharias, J. J. Haslam, T. J. Clancy, M. F. Yeoman, D. P. Warwas, T. C. Sangster, C. Stoeckl, J. P. Knauer, and C. J. Horsfield, Rev. Sci. Instrum. **81**, 10D319 (2010).
[4] V. Y. Glebov, T. C. Sangster, C. Stoeckl, J. P. Knauer, W. Theobald, K. L. Marshall, M. J. Shoup, T. Buczek, M. Cruz, T. Duffy, M. Romanofsky, M. Fox, A. Pruyne, M. J. Moran, R. A. Lerche, J. McNaney, J. D. Kilkenny, M. J. Eckart, D. Schneider, D. Munro, W. Stoeffl, R. Zacharias, J. J. Haslam, T. Clancy, M. Yeoman, D. Warwas, C. J. Horsfield, J. L. Bourgade, O. Landoas, L. Disdier, G. A. Chandler, and R. J. Leeper, Rev. Sci. Instrum. **81**, 10D325 (2010).
[5] A. Bernard, A. Coudeville, A. Jolas, J. Lauspach, and J. de Mascreau, Phys. Fluids **18**, 180 (1975).
[6] I. Tiseanu, G. Decker, and W. Kies, Nucl. Instrum. Methods Phys. Res. A **373**, 73 (1996).
[7] R. Aliaga-Rossel and P. Choi, IEEE Trans. Plasma Sci. **26**, 1138 (1998).
[8] P. Kubes, J. Kravarik, D. Klir, K. Rezac, M. Scholz, M. Paduch, K. Tomaszewski, I. Ivanova-Stanik, B. Bienkowska, L. Karpinski, M. Jan Sadowski, and H. Schmidt, IEEE Trans. Plasma Sci. **34**, 2349 (2006).
[9] C. A. Coverdale, C. Deeney, A. L. Velikovich, J. Davis, R. W. Clark, Y. K. Chong, J. Chittenden, S. Chantrenne, C. L. Ruiz, G. W. Cooper, A. J. Nelson, J. Franklin, P. D. LePell, J. P. Apruzese, J. Levine, and J. Banister, Phys. Plasmas **14**, 056309 (2007).
[10] P. Kubes, D. Klir, J. Kravarik, K. Rezac, IEEE Trans. Plasma Sci. **37**, 1786 (2009).
[11] R. Verma, R. S. Rawat, P. Lee, M. Krishnan, S. V. Springham, and T. L. Tan, Plasma Phys. Controlled Fusion **51**, 075008 (2009).
[12] D. Klir, J. Kravarik, P. Kubes, K. Rezac, J. Cikhardt, E. Litseva, T. Hyhlik, S. S. Ananev, Yu. L. Bakshaev, V. A. Bryzgunov, A. S. Chernenko, Yu. G. Kalinin, E. D. Kazakov, V. D. Korolev, G. I. Ustroev, A. A. Zelenin, L. Juha, J. Krasa, A. Velyhan, L. Vysin, J. Sonsky, and I. V. Volobuev, Plasma Phys. Controlled Fusion **52**, 065013 (2010).
[13] G. F. Knoll, *Radiation Detection and Measurement*, 3rd ed. (Wiley, New York, 1999).
[14] D. Klir, J. Kravarik, P. Kubes, K. Rezac, S. S. Ananev, Yu. L. Bakshaev, P. I. Blinov, A. S. Chernenko, E. D. Kazakov, V. D. Korolev, G. I. Ustroev, L. Juha, J. Krasa, A. Velyhan, IEEE Trans. Plasma Sci. **37**, 425 (2009).
[15] Saint-Gobain Crystals, Scintillation Products, Organic Scintillator. Available: http://www.detectors.saint-gobain.com/uploadedFiles/SGdetectors/Documents/Brochures/Organics-Brochure.pdf.
[16] Hamamatsu, Photomultiplier Tubes. Available: http://sales.hamamatsu.com/assets/pdf/catsandguides/PMT_TPMO0009E01.pdf.
[17] Hamamatsu, Photomultiplier Tube R1828-01. Available: http://sales.hamamatsu.com/assets/pdf/parts_R/R1828-01.pdf.
[18] K. Tomaszewski, in *AIP Conference Proceedings*, *17th IAEA Technical Meeting on Research Using Small Fusion Devices*, Lisbon, 2007 (American Institute of Physics, New York, 2008), Vol. 996, p. 89.
[19] K. Tomaszewski, in *AIP Conference Proceedings*, *16th IAEA Technical Meeting on Research Using Small Fusion Devices*, Mexico, 2005 (American Institute of Physics, New York, 2006), Vol. 875, p. 41.
[20] K. Jungwirth, A. Cejnarova, L. Juha, B. Kralikova, J. Krasa, E. Krousky, P. Krupickova, L. Laska, K. Masek, T. Mocek, M. Pfeifer, A. Präg, O. Renner, K. Rohlena, B. Rus, J. Skala, P. Straka, and J. Ullschmied, Phys. Plasmas **8**, 2495 (2001).
[21] See National Technical Information Service Document No. DE87000708 (J. F. Briesmeister, MCNP: A general Monte Carlo code for neutron and photon transport, LANL Report No. DE87000708, 1986). Copies may be ordered from National Technical Information Service, Springfield, VA.
[22] S. A. Pozzi, J. A. Mullens, J. T. Mihalczo, Nucl. Instrum. Methods Phys. Res. A **524**, 92 (2004).
[23] S. A. Pozzi, M. Flaska, A. Enqvist, and I. Pazsit, Nucl. Instrum. Methods Phys. Res. A **582**, 629 (2007).
[24] D. Klir, J. Kravarik, P. Kubes, K. Rezac, S. S. Ananev, Yu. L. Bakshaev, P. I. Blinov, A. S. Chernenko, E. D. Kazakov, V. D. Korolev, B. R. Meshcherov, G. I. Ustroev, L. Juha, J. Krasa, and A. Velyhan, Phys. Plasmas **15**, 032701 (2008).
[25] A. A Naqvi, A. Aksoy, F. Z. Khiari, A. Coban, M. M. Nagadi, M. A. Al-Ohali, and M. A. Al-Jalal, Nucl. Instrum. Methods Phys. Res. A **345**, 514 (1994).
[26] M. Scholz, L. Karpinski, M. Paduch, K. Tomaszewski, R. Miklaszewski, and A. Szydlowski, Nukleonika **46**, 35 (2001).
[27] L. E. Ruggles, J. L. Porter, W. W. Simpson, M. F. Vargas, D. M. Zagar, R. Hartke, F. Buersgens, D. R. Symes, and T. Ditmire, Rev. Sci. Instrum. **75**, 3595 (2004).
[28] R. Hartke, D. R. Symes, F. Buersgens, L. E. Ruggles, J. L. Porterb, and T. Ditmire, Nucl. Instrum. Methods Phys. Res. A **540**, 464 (2005).
[29] K. Rezac, D. Klir, P. Kubes, J. Kravarik, and M. Stransky, Czech J. Phys. **56**, B357 (2006).

[30]K. Rezac, D. Klir, P. Kubes, J. Kravarik, in *AIP Conference Proceedings, 7th International Conference on Dense Z-Pinches*, Alexandria, VA, 2008 (American Institute of Physics, New York, 2009), Vol. 1088, p. 211.
[31]M. B. Chadwick, P. Obložinský, M. Herman, N. M. Greene, R. D. McKnight, D. L. Smith, P. G. Young, R. E. Macfarlane, G. M. Hale, S. C. Frankle, A. C. Kahler, T. Kawano, R. C. Little, D. G. Madland, P. Moller, R. D. Mosteller, P. R. Page, P. Talou, H. Trellue, M. C. White, W. B. Wilson, R. Arcilla, C. L. Dunford, S. F. Mughabghab, B. Pritychenko, D. Rochman, A. A. Sonzogni, C. R. Lubitz, T. H. Trumbull, J. P. Weinman, D. A. Brown, D. E. Cullen, D. P. Heinrichs, D. P. McNabb, H. Derrien, M. E. Dunn, N. M. Larson, L. C. Leal, A. D. Carlson, R. C. Block, J. B. Briggs, E. T. Cheng, H. C. Huria, M. L. Zerkle, K. S. Kozier, A. Courcelle, V. Pronyaev, and S. C. van der Marck, Nucl. Data Sheets **107**, 2931 (2006).
[32]M. J. Bernstein and G. G. Comisar, Phys. Fluids **15**, 700 (1972).
[33]D. R. Welch, D. V. Rose, C. Thoma, R. E. Clark, C. B. Mostrom, W. A. Stygar, and R. J. Leeper, Phys. Plasmas **17**, 072702 (2010).
[34]M. Scholz, B. Bienkowska, I. M. Ivanova-Stanik, L. Karpinski, M. Paduch, E. Zieliñska, J. Kravarik, P. Kubes, M. J. Sadowski, and A. Szydlowski, H. Schmidt, Czech. J. Phys. Suppl. B **56**, 243 (2006).
[35]J. Krasa, M. Kralik, A. Velyhan, J. Solc, L. Juha, M. Scholz, B. Bienkowska, I. M. Ivanova-Stanik, L. Karpinski, R. Miklaszewski, M. Paduch, H. Schmidt, K. Tomaszewski, D. Klir, J. Kravarik, P. Kubes, and K. Rezac, Plasma Phys. Controlled Fusion **50**, 125006 (2008).
[36]D. Klir, P. Kubes, M. Paduch, T. Pisarczyk, T. Chodukowski, M. Scholz, Z. Kalinowska, E. Zielinska, B. Bienkowska, J. Hitschfel, S. Jednorog, L. Karpinski, J. Kortanek, J. Kravarik, K. Rezac, I. Ivanova-Stanik, and K. Tomaszewski, Appl. Phys. Lett. **98**, 071501 (2011).
[37]M. Králík, J. Krása, A. Velyhan, M. Scholz, I. M. Ivanova-Stanik, B. Bienkowska, R. Miklaszewski, H. Schmidt, K. Řezáč, D. Klír, J. Kravárik, and P. Kubeš, Rev. Sci. Instrum. **81**, 113503 (2010).